

Vertical and Adiabatic Ionization Energies and Electron Affinities of New Si_nC and Si_nO ($n = 1-3$) Molecules

Alexander I. Boldyrev and Jack Simons*

Department of Chemistry, The University of Utah, Salt Lake City, Utah 84112

Vyacheslav G. Zakrzewski† and Wolfgang von Niessen

Institut für Physikalische und Theoretische Chemie, Technische Universität Braunschweig, Hans-Sommer Strasse 10, D-3300 Braunschweig, Germany

Received: August 27, 1993*

Vertical and adiabatic ionization potentials (IPs) as well as electron affinities have been calculated for SiC , Si_2C , Si_3C , SiO , Si_2O , and Si_3O using five different sophisticated ab initio methods with large basis sets. The geometry and harmonic frequencies have been calculated at the second-order Møller–Plesset level. Results of the calculations using all five methods are in a good agreement among themselves (± 0.5 eV). The calculated vertical first IPs of SiC , Si_2C , Si_3C , and SiO molecules agree within 0.2 eV with experimental appearance potentials for these species.

Introduction

Recently, silicon–carbon (Si_nC) and silicon–oxygen (Si_nO) ($n = 2,3$) molecular clusters have been studied theoretically.^{1,2} Geometrical structures and vibrational frequencies for the ground electronic states have been obtained for Si_2C and Si_3C that agree well with the available experimental data. In this study, we present ab initio calculations at several levels of theory for vertical and adiabatic ionization potentials and vertical and adiabatic electron affinities for Si_nC and Si_nO ($n = 1-3$). These data may be valuable for future mass spectrometric and spectroscopic studies because several of these molecules have not been experimentally observed. Hence, theoretically predicted appearance potentials may be helpful for guiding experimental detection. To achieve as reliable results as possible, we have used several methods (Møller–Plesset perturbation theory (MPn), quadratic configuration interaction (QCISD(T)), conventional configuration interaction (CISD), and Green function methods (the OVGf and ADC(3) approaches discussed below)) and different types of atomic basis sets in performing the calculations whose results are reported here.

Computational Details

The bond lengths of the neutral, cationic, and anionic SiC , Si_2C , Si_3C , SiO , Si_2O , and Si_3O species were optimized by employing analytical gradients³ using the Gaussian 92 program⁴ with polarized split-valence basis sets (6-311+G*)⁵⁻⁷ at MP2-(full) levels (UMP2(full) for open shell systems). Our optimal geometric parameters are presented in Figure 1, and our simulated IR spectra based on the MP2(full)/6-311+G* calculated frequencies are drawn in Figure 2. The MP2(full)/6-311+G* equilibrium geometries were used to evaluate electron correlation corrections in the frozen-core approximation by full fourth-order⁸ Møller–Plesset perturbation theory and by the (U)QCISD(T) method⁹ using 6-311+G(2df) basis sets. The UHF wave functions for open shell systems were projected to pure spectroscopic states for which the corresponding results are denoted PUSCF, PMP2, PMP3, and PMP4.¹⁰

The vertical ionization energies and electron affinities were also calculated by two approximations to the many-body one-particle Green function,¹¹⁻¹⁶ namely, the outer valence Green

function (OVGF) and the third-order algebraic diagrammatic construction (ADC(3)).

In the OVGf method, all the diagrams up to and including the third-order terms which appear in the expansion of the self-energy are included, and a renormalization procedure is used for the higher order corrections.¹¹⁻¹³ The renormalization procedure includes three cases described in detail in ref 15 and represents a geometric-type approximation to the self-energy. Usually the approximation denoted case b in ref 15 was chosen. Whenever the OVGf approximation was applicable, all three procedures yielded very similar results.

The ADC(3) method takes all one-hole, one-particle, two-hole + one-particle, and two-particle + one-hole configurations and their interactions into account. Contributions from so-called constant or energy-independent diagrams were evaluated by the iterative procedure of ref 16. The value of the pole strengths (the residues of the Green function at each pole) are also calculated within the Green function method and measure the validity of the one-particle picture of ionization (or electron capture). The electron correlation effects make processes other than the simplest Koopmans' theorem ionization events available, in which case the pole strengths are no longer equal to unity but remain close to unity when the one-particle picture of ionization (or attachment) remains valid. When complete breakdown of the one-particle description occurs, the pole strengths are much smaller than unity, and instead of one photoelectron line, there appear a number of additional lines known as shake-up (or shake-off) satellites.

The SCF calculations preceding the OVGf and ADC(3) calculations employed the MOLCAS-2 suite of programs.¹⁷ For these calculations, we used the very large ANO basis set of Widmark et al.¹⁸ For the Si atom, this consists of (17s12p5d4f) elementary functions and [6s5p2d1f] contracted functions, and for the C and O atoms, (14s9p4d3f) elementary and [4s3p2d1f] contracted functions. The ANO basis set is especially suited for the calculation of properties where an extensive correlation treatment is necessary and an extended basis set including diffuse functions is required. It involves minimal contraction loss.¹⁹ (The so-called general contraction scheme is used in these ANO basis sets where all elementary functions enter each contracted function). These basis sets are probably the best for the precise calculation of ionization potentials and electron affinities.

The vertical and adiabatic ionization energies and electron affinities were also calculated for the lowest cationic and anionic states using single-reference single- and -double-excitation CI

* Present address: Department of Chemistry, University of New Mexico, Albuquerque, NM 87131.

† Abstract published in *Advance ACS Abstracts*, December 15, 1993.

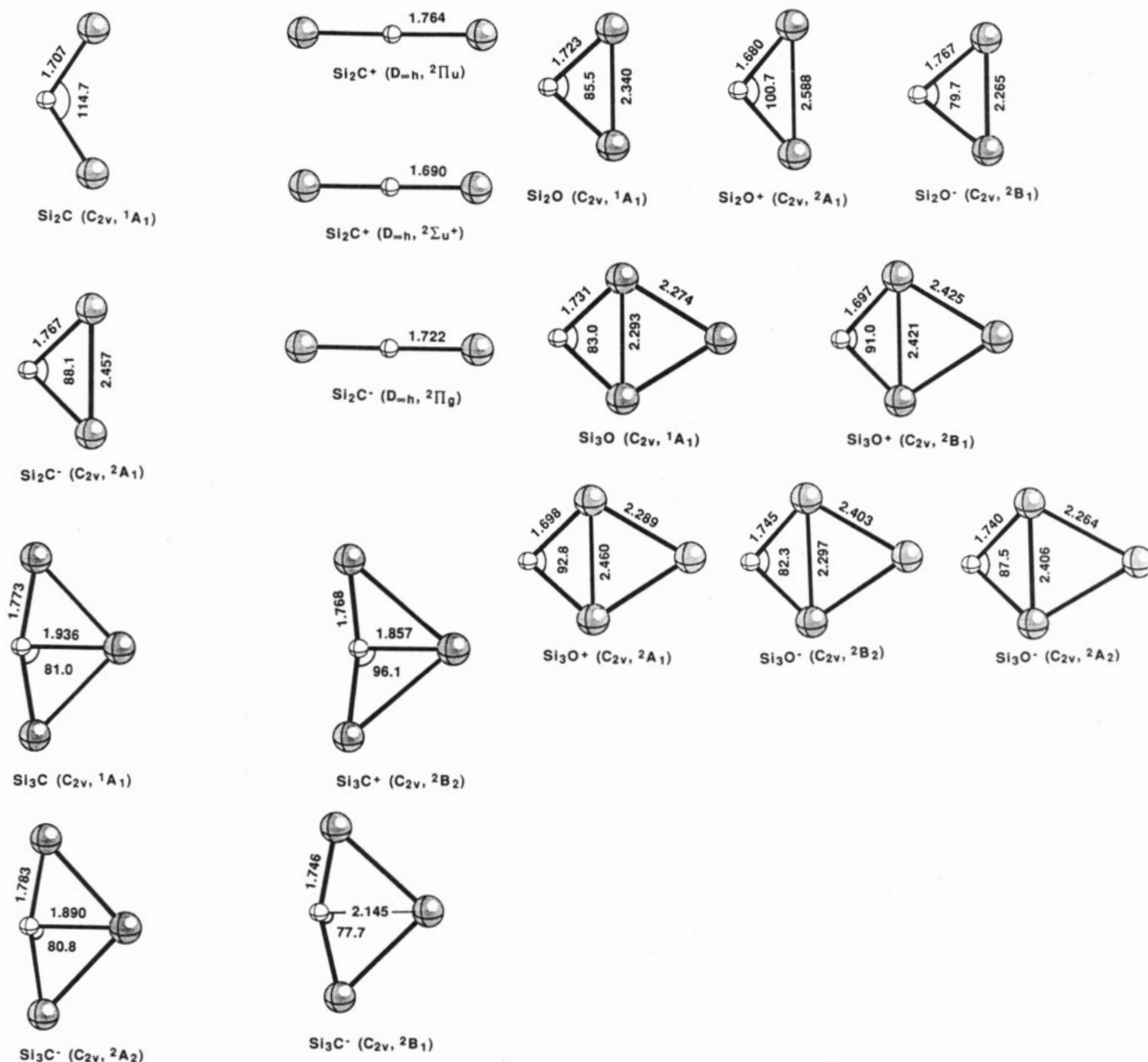


Figure 1. Molecular structures and geometrical parameters (distances in angstroms and angles in degrees) at the MP2(full)/6-311+G* level for Si₂C, Si₂C⁺, Si₂C⁻, Si₂O, Si₂O⁺, Si₂O⁻, Si₃C, Si₃C⁺, Si₃C⁻, Si₃O, Si₃O⁺, and Si₃O⁻.

(CISD). The CISD energies were corrected by the Davidson method²⁰ (CISD(4)) to account for the quadruple and higher order excited configurations. These calculations were also performed using the MOLCAS-2 program, where only the core orbitals were kept frozen in all the Green function and CISD calculations. The final estimates for the vertical and adiabatic ionization potentials and electron affinities are made by averaging the data at the PMP4, QCISD, CISD, OVGf, and ADC(3) levels, and \pm values are assigned to the range of energies predicted by the various methods.

Results and Discussion

SiC, SiC⁺, and SiC⁻. The neutral SiC molecule is known to have a triplet ³Π_i (1σ²2σ²1π³3σ¹) ground electronic state.^{21,22} Our calculated bond length $R_e(\text{Si-C}) = 1.702$ Å and harmonic frequency $\nu_e = 896$ cm⁻¹ agree reasonably with experimental data: $R_e(\text{Si-C}) = 1.722$ Å²¹ and $\nu_e = 964.6$ cm⁻¹.²¹ An experimental appearance potential has been determined for SiC: 9.2 ± 0.4 eV in ref 23 and 9.0 eV in ref 24. We were not able to find in the literature any data on the electronic state, bond lengths, or vibrational frequencies of the positive and negative ions of SiC.

From the ground electronic state we can expect two low-energy cationic states: ⁴Σ⁻(1σ²2σ²1π²3σ¹) and ²Π_i(1σ²2σ²1π³) for SiC⁺, when an electron is removed from the highest σ- or π-MO. We examined these two states as well as the ²Σ⁺(1σ²2σ²1π⁴) state. A simple MO picture of the valence MOs suggests the following: 1σ-MO is bonding (s_C + s_{Si}), 2σ-MO is antibonding (s_C - s_{Si}), 1π-MO is bonding (p_{x,y,C} + p_{x,y,Si}), and 3σ-MO is bonding (p_{z,C} - p_{z,Si}). From this simple picture we expect that the detachment of an electron either from the bonding 1π-MO (to give the ⁴Σ⁻ final state) or from the bonding 3σ-MO (yielding the ²Π_i final state) should increase the Si-C bond length and decrease the vibrational frequency. In contrast, detachment of an electron from the antibonding 2σ-MO accompanied by promotion of an electron from 3σ-MO into the 1π-MO (to give the ²Σ⁺ final state) should sharply decrease the Si-C bond length and increase the vibrational frequency. This trend is found in our calculations (see below results for SiC and SiO), but not in all cases.

The energy order of the ionic states is not easy to predict from the simple MO picture. The ⁴Σ⁻ state is found to be the lowest cationic state. The ²Π_i and ²Σ⁺ states are 2.5 and 5.3 eV higher at the PMP4/6-311+G(2df) level. The optimized bond lengths and frequencies are 1.804 Å and 890 cm⁻¹ for ⁴Σ⁻, 1.675 Å and 952 cm⁻¹ for ²Π_i, and 1.504 Å and 1443 cm⁻¹ for ²Σ⁺. We estimate

the first vertical IP_v = 8.9 ± 0.2 eV (IP = ionization potential) for producing ⁴Σ⁻ SiC⁺ to be in the range 8.8 eV (PMP4), 9.0 eV (QCISD(T)), and 9.0 eV (CISD(4)), which agrees well with the experimental appearance potentials 9.2 ± 0.4 eV²³ and 9.0 eV.²⁴ Our first adiabatic IP_a is 8.7 ± 0.2 eV.

The experimental electron affinity is not known for SiC; therefore, our data may help in the identification of SiC⁻ anions. The two lowest anion electronic states ²Π_i(1σ²2σ²1π³3σ²) and ²Σ⁺(1σ²2σ²1π⁴3σ¹) may be derived from the ground electronic state of neutral SiC when an electron is added to the lowest energy available MOs. Again, from the MO picture, one expects that bond lengths and vibration frequencies should decrease and increase, respectively, for both anionic states.

The ²Σ⁺ is found to be the lowest of SiC⁻; however, the ²Π_i state lies only 0.4 eV (QCISD(T)/6-311+G(2df)) above the ²Σ⁺ ground state. The optimized bond lengths and vibrational frequencies are 1.759 Å and 1127 cm⁻¹ for ²Σ⁺ and 1.710 Å and 951 cm⁻¹ for ²Π_i. Both of these states are lower than the neutral SiC molecule, so this molecule has two bound negative ion states. The first adiabatic electron affinity of SiC is 2.25 eV, which differs slightly from the vertical EA_v = 2.32 eV (EA = electron affinity). Although EA(SiC) is very high, it is lower than EA(C₂) = 3.269 ± 0.006 eV^{25a} and EA(C₂) = 3.273 ± 0.008 eV^{25b} and close to EA(Si₂) = 2.176 ± 0.002 eV^{26a} and EA(Si₂) = 2.199 ± 0.012 eV.^{26b} The SiC⁻ ion also has an excited bound ²Π_i state which lies below the ground ³Π state of SiC by 1.83 eV and thus may be found in the gas-phase experiments. The next ²Π_r state of SiC⁻ with 1σ²2σ²1π⁴2π¹ orbital occupancy is not electronically bound and corresponds to a resonance lying above the energy of the neutral SiC by 1.8 eV.

Si₂C, Si₂C⁺, and Si₂C⁻. The neutral Si₂C molecule is one of the major molecular species (8%) observed in mass spectrometric studies of the vaporization of silicon carbide.²³ In the first infrared work, Weltner and McLeod²⁷ proposed the tentative assignment to Si₂C of a vibration observed at 1187 and 1205 cm⁻¹ in spectra of the products of silicon carbide evaporation trapped in Ar and Ne matrices, respectively. Later, Kafafi et al.²⁸ obtained ¹³C data which led them to assign two absorptions at 1188.9 and 658.2 cm⁻¹, which shifted to 1153.7 and 643.3 cm⁻¹, respectively, and appeared to grow in with the same relative intensity, to the ν₃(b₂) antisymmetric Si–C stretching and ν₁(a₁) symmetric Si–Si stretching modes, respectively, of Si₂C. Finally, a Fourier transform infrared study of the vibrational spectrum of Si₂C produced by vaporizing a mixture of silicon and carbon-12 or carbon-13 has been made by Presilla–Márquez and Graham.²⁹ This confirmed a previously observed vibration at 1188.4 cm⁻¹ as the ν₃(b₂) antisymmetric Si–C stretching mode, and resulted in the identification of a new vibration at 839.5 cm⁻¹ as the ν₁(a₁) symmetric Si–Si stretching fundamental. No bending mode has been observed. Ab initio calculations performed by Grev and Schaefer,^{1a} Bolton et al.,^{1b} and Rittby^{1c} predicted a singlet angular C_{2v}(¹A₁) structure for Si₂C. However, the predicted equilibrium angle Si–C–Si is very sensitive to the basis set¹ because this molecule is very floppy with a barrier for linearity of only 1.9^{1c} or 2.1^{1a} kcal/mol. Experimental appearance potentials are known for Si₂C, 9.2 ± 0.3 eV²³ and 9.1 eV,²⁴ but no electronic, geometric, or vibrational data are available for the cationic or anionic states of Si₂C.

We optimized the geometry for the neutral Si₂C and obtained R_e(Si–C) = 1.707 Å, valence angle Si–C–Si = 114.7° and harmonic frequencies ν₁(a₁) = 844 cm⁻¹, ν₂(a₁) = 129 cm⁻¹, and ν₃(b₂) = 1208 cm⁻¹. Our bond length and valence angle reasonably agree with other CCSD(T)/TZ+2P (1.708 Å and 116.9°)^{1b} and MBPT2/6-311G(2d) (1.703 Å and 119.5°)^{1c} ab initio data if we take into account the flexible structure of this species. Our harmonic symmetric and antisymmetric stretching frequencies ν₁(a₁) = 844 cm⁻¹ and ν₃(b₂) = 1208 cm⁻¹ also reasonably agree

with experimental data, ν₁(a₁) = 839.5 cm⁻¹³⁰ and ν₃(b₂) = 1188.9 cm⁻¹.²⁹

From the 1a₁²1b₂²2a₁²2b₂²1b₁²3a₁²1a₂⁰4a₁⁰ ground electronic SCF configuration, we found in OVGf and ADC(3) calculations that the lowest energy cationic states are ²A₁(1a₁²1b₂²2a₁²2b₂²1b₁²3a₁¹), ²B₁(1a₁²1b₂²2a₁²2b₂²3a₁²1b₁¹), and ²B₂(1a₁²1b₂²2a₁²1b₁²3a₁²2b₂¹) and the lowest anionic states are ²A₂(1a₁²1b₂²2a₁²2b₂²1b₁²3a₁²1a₂¹) and ²A₁(1a₁²1b₂²2a₁²2b₂²1b₁²3a₁²4a₁¹).

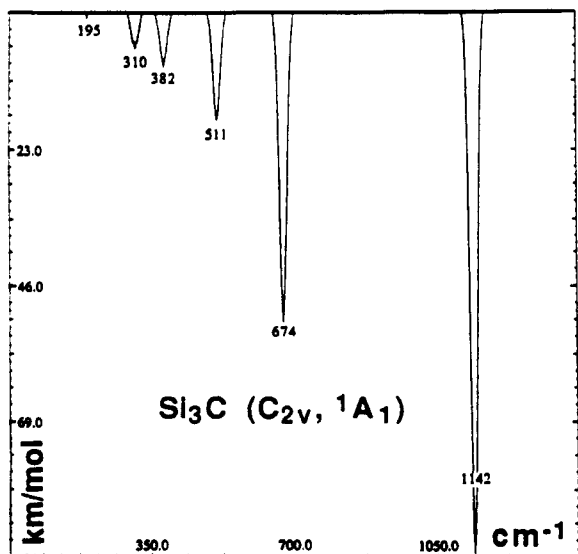
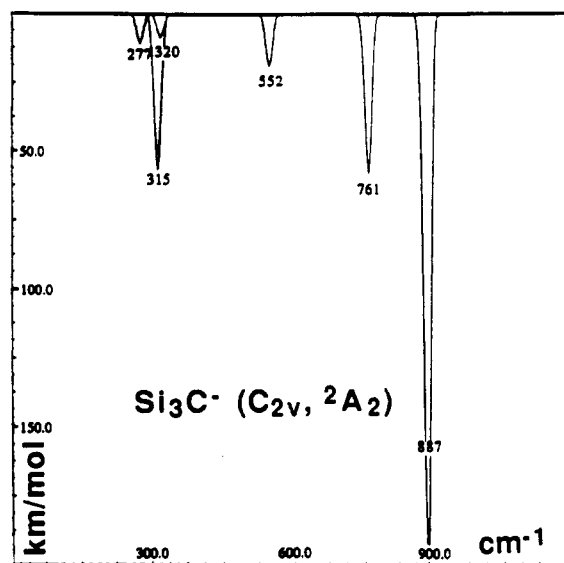
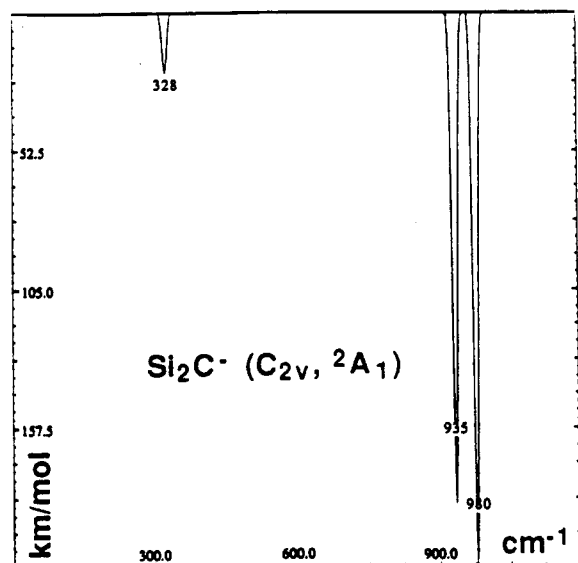
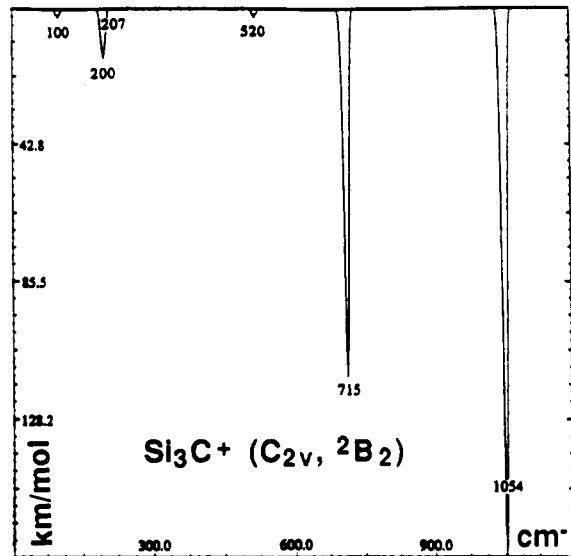
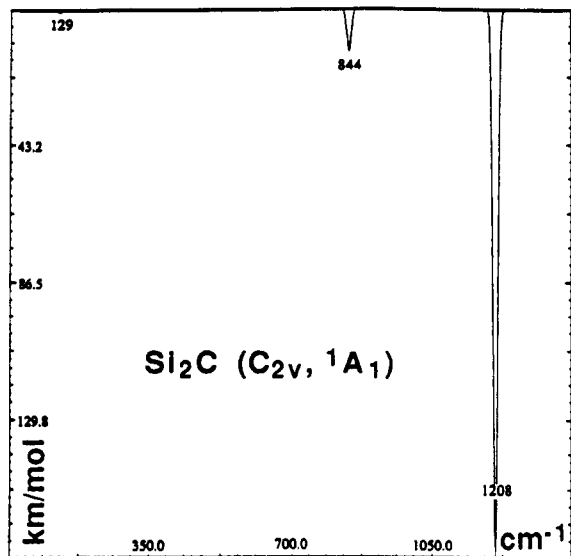
In Koopmans' approximation, the energy order of the cationic states is given as ²A₁ < ²B₁ < ²B₂. However, as shown in Table 1, at all correlated levels and even at the ΔSCF level, the order of the cationic states is different: ²B₂ < ²A₁ < ²B₁. Results of the calculations of the vertical IPs obtained at correlated levels agree within 0.25 eV for all give methods: ΔMP4, ΔQCISD(T), ΔCISD(4), OVGf, and ADC(3). On the basis of these data, we estimate the vertical ionization potentials to be IP(²B₂) = 9.1 ± 0.2 eV, IP(²A₁) = 9.3 ± 0.2 eV, and IP(²B₁) = 9.4 ± 0.2 eV. The first vertical IP agrees well with the experimental appearance potential for Si₂C, 9.2 ± 0.3 eV²³ and 9.1 eV.²⁴

All of these ²A₁, ²B₁, and ²B₂ states are well represented by one-configuration wave functions in which the coefficients of the Hartree–Fock determinant in CISD calculations are larger than 0.9 and the pole strengths in the OVGf and ADC(3) calculations are ca. 0.9. However, the higher ionic states with ionization energy larger than 12 eV are not well represented as the ionization from a single MO (see Table 1). For example, ionization from the next 2a₁-MO of Si₂C with orbital energy 12.33 eV is accompanied by strong many-body effects. Three peaks may occur in the photoelectron spectrum according to the ADC(3) calculations (see Table 1) while the configuration of the 2a₁⁻¹ final state remains strong (11.19 eV) and has a relative intensity of 0.67. The remainder of the intensity is shared by satellite lines, among which there is one line at 13.36 eV with a relative intensity of 0.15 (see Table 1).

Geometry optimization of the ²A₁, ²B₁, and ²B₂ states of Si₂C⁺ leads to a linear SiCSi structure. The ²A₁ and ²B₁ states collapse into the degenerate ²Π_u(1σ_g²1σ_u²2σ_g²2σ_u²1π_u³) state, and the ²B₂ state collapses into the ²Σ_u⁺(1σ_g²1σ_u²2σ_g²1π_u⁴2σ_u¹). For both of these linear states, the optimal geometries are presented in Figure 1, and the corresponding adiabatic ionization potentials, IP_a(²Π_u) and IP_a(²Σ_u⁺), are equal to 9.0 ± 0.2 and 9.2 ± 0.2 eV, respectively. Harmonic frequencies have been calculated only for the ²Σ_u⁺ state. As a result, even though ν₁(σ_g) = 584 cm⁻¹ and ν₂(π_u) = 92 cm⁻¹ appear reasonable, the antisymmetric stretching frequency ν₃(σ_u) = 2405 cm⁻¹ is too high, probably due to symmetry breaking.

The lowest unoccupied 1a₂- and 4a₁-MOs in Si₂C have positive energies at the optimal geometry of the neutral Si₂C molecule; therefore, at Koopmans' approximation these states do not have positive vertical electron affinities. However, when correlation and electron relaxation are taken into account, both of these states become bound. The vertical EA_vs of Si₂C calculated for the ²A₂ and ²A₁ states are 0.6 ± 0.2 eV and 0.1 ± 0.2 eV, respectively. Geometry optimization of the ²A₂ state leads to a linear structure and a ²Π_g final electronic state, while the final geometric structure of the ²A₁ state is bent. Moreover, in the Si₂C⁻(²A₁) structure the silicon–silicon distance is very short (2.46 Å) and only 0.13 Å larger than a normal single Si–Si bond length. We therefore infer that Si₂C⁻(²A₁) has significant Si–Si bonding. The calculated IR spectrum of Si₂C⁻(²A₁) is presented in Figure 2. The adiabatic electron affinities for producing the two anion states, EA_a(²Π_g) and EA_a(²A₁), are 0.9 ± 0.2 and 0.7 ± 0.2 eV, respectively.

Si₃C, Si₃C⁺, and Si₃C⁻. This molecule has been detected in mass spectroscopic experiments, and an appearance potential of 8.2 ± 0.3 eV has been reported.²³ The experimental spectrum of Si₃C has been observed³⁰ in a Fourier transform infrared study



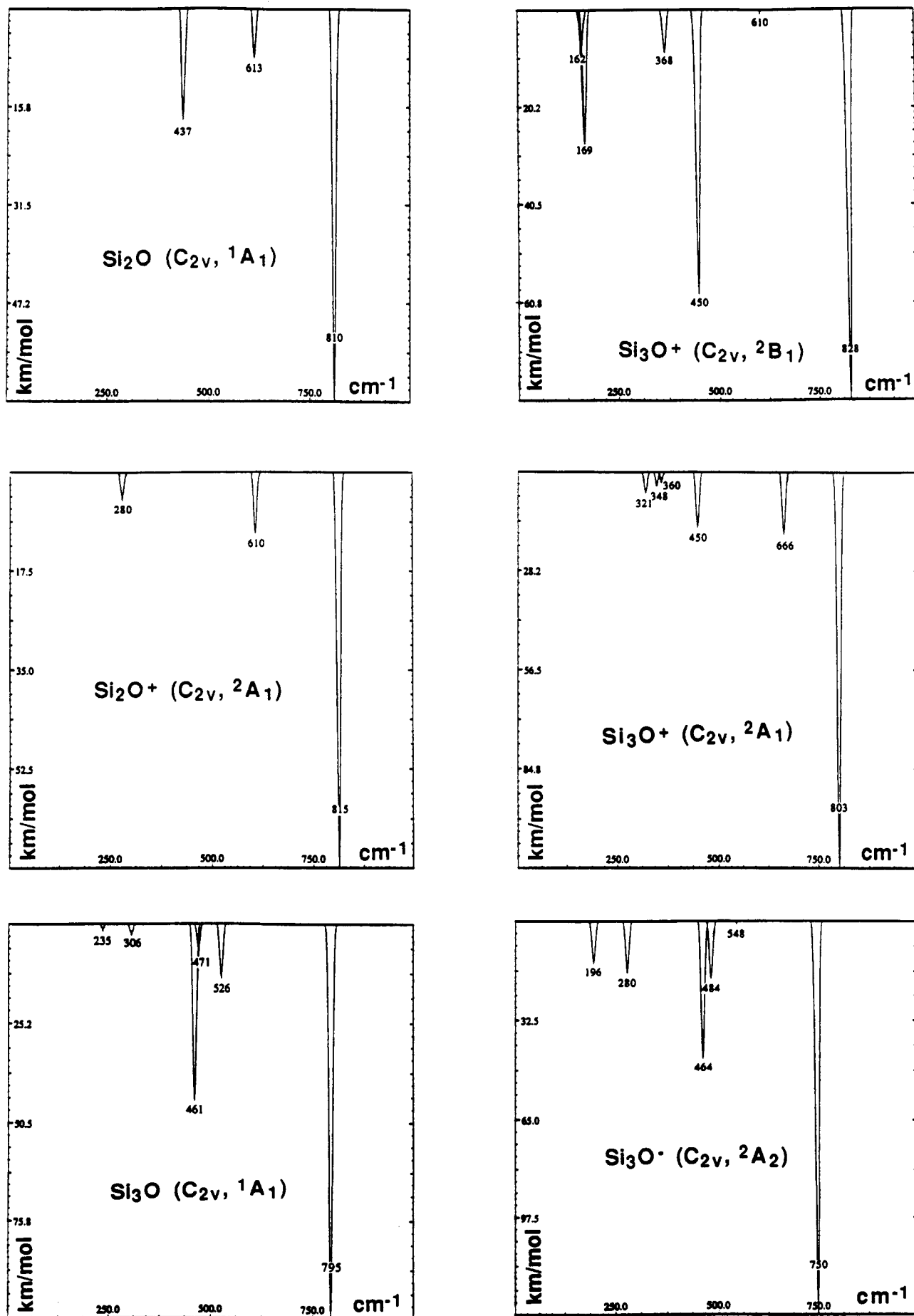


Figure 2. Calculated infrared absorption spectra for Si₂C, Si₂C⁺, Si₂C⁻, Si₂O, Si₂O⁺, Si₂O⁻, Si₃C, Si₃C⁺, Si₃C⁻, Si₃O, Si₃O⁺, and Si₃O⁻.

TABLE 1: Calculated and Experimental Ionization Potentials and Electron Affinities of Si_nO and Si_nC Molecules

ionic species	state	IP/EA	Koopmans' approximation	ΔPUSCF	ΔPMP2	ΔPMP3	ΔPMP4	ΔQCISD(T)	ΔCISD + Davidson correction	OVGF ^a	ADC(3) ^a	exptl
SiO ⁺	² Σ ⁺	IP _v	16.58							15.57 (0.95)		
SiO ⁺	² Π _i	IP _v	12.76	9.70	12.27	11.52	12.19	11.96	11.74	12.26 (0.92)	12.21 (0.88)	
		IP _a		9.57	12.02	11.30	11.92	11.70	11.45			
SiO ⁺	² Σ ⁺	IP _v	11.94	10.15	12.01	11.55	11.91	11.48	11.51	11.92 (0.93)	11.66 (0.90)	11.6 ± 0.2 ^b 11.43 ^c
		IP _a		10.15	12.01	11.55	11.91	11.48	11.51			
SiO ⁻	² Π _r	EA _v	-0.59	-0.34	-0.18	-0.04	-0.20	-0.14		-0.06		
		EA _a		-0.24	-0.15	-0.07	-0.15	-0.12				
Si ₂ O ⁺	² A ₁	IP _v	12.77								11.44 (0.59) 12.07 (0.21) 10.18 (0.71) 11.56 (0.15)	
Si ₂ O ⁺	² B ₂	IP _v	11.00	9.71	10.68	10.69	10.68					
Si ₂ O ⁺	² Π _g	IP ₂		6.00	7.23	7.18	7.39	7.37				
Si ₂ O ⁺	² A ₁	IP _v	7.36	6.93	7.39	7.53	7.56	7.58	7.50	7.57 (0.90)	7.29 (0.89)	
		IP _a		6.00	7.21	7.21	7.37	7.34	7.22			
Si ₂ O ⁻	² B ₁	EA _v	-0.04	0.48	0.99	0.97	0.98	0.95	0.87	0.88 (0.92)	0.82 (0.85)	
		EA _a		0.51	1.08	1.02	1.07	1.01	0.94			
Si ₃ O ⁺	² B ₂	IP _v	12.32								10.92 (0.28) 11.54 (0.43) 11.96 (0.03) 13.43 (0.07)	
Si ₃ O ⁺	² A ₁	IP _v	10.93							10.49 (0.85)	10.12 (0.80)	
Si ₃ O ⁺	² A ₁	IP _v	8.77	7.64	8.83	8.79	8.88			8.72 (0.88)	8.41 (0.86)	
		IP _a		7.48	8.53	8.47	8.58					
Si ₃ O ⁺	² B ₁	IP _v	8.06	7.13	8.26	8.17	8.27		8.07	8.14 (0.89)	7.86 (0.88)	
		IP _a		6.55	8.00	7.77	7.97		7.68			
Si ₃ O ⁻	² B ₂	EA _v	0.77	1.63	1.40	1.54	1.38		1.62	1.55 (0.90)	1.39 (0.85)	
		EA _a		1.76	1.73	1.79	1.70		1.71			
Si ₃ O ⁻	² A ₂	EA _v	-0.40	0.74	0.65	0.69	0.73		0.60	0.52 (0.91)	0.43 (0.85)	
		EA _a		0.84	0.74	0.79	0.81		0.68			
SiC ⁺	² Σ ⁺	IP _v		13.36	14.37	14.47	14.39		14.17			
		IP _a		14.02	13.91	14.08	13.98	13.92	14.10			
SiC ⁺	² Π _i	IP _v		11.22	10.39	10.47	10.22	10.13	10.15			
		IP _a										
SiC ⁺	⁴ Σ ⁻	IP _v		7.95	8.72	8.73	8.85	8.97				9.2 ± 0.4 ^d 9.0 ^e
		IP _a		7.85	8.57	8.57	8.68	8.78				
SiC ⁻	² Π _i	EA _v		0.15	2.14	1.97	2.15	1.82	1.73			
		EA _a		0.52	1.94	1.87	2.00	1.83	1.71			
SiC ⁻	² Σ ⁺	EA _v		0.07	2.48	2.06	2.22	2.32	2.05			
		EA _a		-0.10	2.54	2.01	2.58	2.25	2.00			
Si ₂ C ⁺	² A ₁	IP _v	12.33								11.19 (0.67) 13.36 (0.15) 15.58 (0.02)	
Si ₂ C ⁺	² B ₂	IP _v	9.70	8.32	9.13	9.18	9.16	9.14	9.22	9.33 (0.89)	9.06 (0.86)	9.2 ± 0.3 ^d 9.1 ^e
	² Σ _u ⁺	IP _a		8.61	9.13	9.28	9.17					
Si ₂ C ⁺	² B ₁	IP _v	9.41	7.84	9.68	9.25	9.60		9.30	9.56 (0.88)	9.31 (0.87)	
	² Π _u	IP _a		<i>f</i>					8.98			
Si ₂ C ⁺	² A ₁	IP _v	9.38	7.47	9.55	9.22	9.52	9.37	9.29	9.45 (0.88)	9.19 (0.86)	
	² Π _u	IP _a							8.98			
Si ₂ C ⁻	² A ₂	EA _v	-0.36	0.94	0.55	0.69	0.67	0.71	0.87	0.55 (0.92)	0.48 (0.87)	
	² Π _g	EA _a			<i>g</i>				0.90			
Si ₂ C ⁻	² A ₁	EA _v	-0.89	-0.30	0.09	0.07	0.15	0.13	-0.21	-0.13 (0.93)		
		EA _a		0.06	0.77	0.73	0.80	0.75	0.65			
Si ₃ C ⁺	² A ₁	IP _v	12.24								10.92 (0.62) 11.87 (0.02) 12.18 (0.08) 13.33 (0.04)	
Si ₃ C ⁺	² B ₁	IP _v	10.42							10.43 (0.88)	10.20 (0.86)	
Si ₃ C ⁺	² B ₂	IP _v	10.09						9.53 (0.88)	9.24 (0.85)		
Si ₃ C ⁺	² A ₁	IP _v	9.14							9.00 (0.88)	8.78 (0.86)	
Si ₃ C ⁺	² B ₂	IP _v	8.08	6.94	8.26	8.14	8.29		8.14	8.29 (0.89)	7.95 (0.87)	8.2 ± 0.3 ^d
		IP _a		6.59	8.03	7.81	8.02		7.80			
Si ₃ C ⁻	² A ₂	EA _v	0.21	1.13	1.43	1.35	1.47		1.28	1.28 (0.91)	1.38 (0.85)	
		EA _a		1.12	1.43	1.36	1.47		1.28			
Si ₃ C ⁻	² B ₁ ^h	EA _v	-0.80	0.01	0.48	0.36	0.48		0.33	0.17 (0.92)		
		EA _a		0.36	0.71	0.65	0.75		0.61			

^a In parentheses are given the pole strengths (see text). ^b Data from ref 32. ^c Data from ref 33. ^d Data from ref 23. ^e Data from ref 24. ^f Optimization at MP2(full)/6-311+G* converged to *D*_{∞h} (²Π_u) structure. ^g Optimization at MP2(full)/6-311+G* converged to *D*_{∞h} (²Π_g) structure. ^h The Si₃C⁻ (*C*_{2v}, ²B₁) structure is not a minimum; therefore, the adiabatic presented EA should be considered as an estimate (see text for details).

of the products of the vaporization of carbon/silicon mixtures trapped in Ar. An ab initio structure of the Si₃C has been determined by Rittby^{1d} at the MBPT2/DZP level, where a rhomboid singlet structure of *C*_{2v} symmetry with carbon-silicon transannular bonding between the two equivalent Si_b (Si_b and Si_i correspond to nearest and remote silicon atoms, respectively)

atoms has been found. The ab initio vibrational spectrum of this structure by Rittby is in excellent agreement with the experimental data of Presilla-Márquez and Graham.³⁰ No experimental or theoretical geometries or vibrational spectra are known for cationic or anionic states of Si₃C thus far.

We optimized the geometry and calculated harmonic fre-

quencies for singlet ($1a_1^2 1b_2^2 2a_1^2 3a_1^2 1b_1^2 2b_2^2 4a_1^2 3b_2^2 1a_2^2 0b_1^0$) rhomboid neutral Si₃C (this geometry is shown in Figure 1). Our geometry and vibrational spectrum (Figure 2) for this structure agree well with the MBPT2/DZP optimized geometry and corresponding vibrational spectrum by Rittby.^{1d}

We studied one cationic state, 2B_2 ($1a_1^2 1b_2^2 2a_1^2 3a_1^2 1b_1^2 2b_2^2 - 4a_1^2 3b_2^1$), which should be the lowest positive ion according to the vertical IPs calculated at the OVGf and ADC(3) levels. The $3b_2$ -MO does not contain contributions from carbon AOs, and has antibonding overlap between AOs from the bridged silicon atoms; however, it has a strong bonding interaction between the terminal and bridged silicons. Therefore, detachment of an electron from the $3b_2$ -MO should lead to a distortion in which an increase of the Si_i-Si_b bonds might be expected. Indeed, geometry optimization for the 2B_2 state of Si₃C⁺ leads to a structure where the Si_b-Si_i distance increases and the valence angle Si_i-CSi_b increases from 81° to 96° (the geometries are shown in Figure 1, and the simulated IR spectra are presented in Figure 2).

We achieved agreement for both vertical IPs (2B_2 and 2A_1) within 0.3 eV for the four different theoretical approaches used: ΔPMP4, ΔCISD(4), OVGf, and ADC(3). From these four methods our best estimates of the two vertical IPs are 8.2 ± 0.2 eV (2B_2) and 9.1 ± 0.2 eV (2A_1). The first IP agrees well with the experimental appearance potential of 8.2 ± 0.3 eV.²³ The geometry of the 2B_2 state differs significantly from the neutral molecule; therefore, the Franck-Condon factor for this ionization process should be rather small although the adiabatic correction (0.4 eV) to the IP is not large (the corresponding adiabatic IP (2B_2) is 7.8 ± 0.2 eV (from PMP4 and CISD(4))).

Based on the MO energy ordering and results of our OVGf and ADC(3) calculations, we found two low-energy anionic states: 2A_2 ($1a_1^2 1b_2^2 2a_1^2 3a_1^2 1b_1^2 2b_2^2 4a_1^2 3b_2^2 1a_2^1$) and 2B_1 ($1a_1^2 - 1b_2^2 2a_1^2 3a_1^2 1b_1^2 2b_2^2 4a_1^2 3b_2^2 2b_1^1$). The orbital energy is negative for the $1a_2$ -LUMO and positive for the $2b_1$ -MO. Both $1a_2$ - and $2b_1$ -MOs are pure π -type orbitals. The $1a_2$ -MO is antibonding with respect to Si_b-Si_i interaction, but because these two atoms are situated far from each other, occupation of this MO should not lead to any essential geometrical changes. The $2b_1$ -MO is antibonding with respect to C-Si_i interaction, so elongation of the C-Si_i bond might be expected in the corresponding anion. As shown in Figure 1, these types of distortions have been found upon geometry optimization. The vertical electron affinities of these two states, EA_v, are estimated to be 1.3 ± 0.2 and 0.3 ± 0.2 eV for the 2A_2 and 2B_1 states, respectively. Geometry optimization does not significantly change the geometry of the Si₃C⁻ (2A_2) state as expected; so the adiabatic EA_a = 1.4 ± 0.2 eV is very close to the vertical electron affinity. The optimal geometry of Si₃C⁻ (2B_1) is very different from the optimal neutral geometry (mainly because of the C-Si_i bond elongates by 0.26 Å), so after geometry relaxation within C_{2v} symmetry the EA (2B_1) = 0.7 eV is higher than the vertical EA. However, frequency calculations for Si₃C⁻ (C_{2v}, 2B_1) have shown that this structure is not a minimum but a saddle point (with one imaginary frequency). The vector belonging to this imaginary frequency leads to an in-plane distortion. Beginning with a geometry slightly distorted from C_{2v} (2B_1) symmetry, we refined the geometry optimization within C_s symmetry. This optimization leads to a C_{2v} (2A_2) structure. With our current computational tools we are not able to find excited states for the negative Si₃C⁻ ion, but we expect the existence of an excited state on the basis of our calculations in the framework of C_{2v} symmetry.

SiO, SiO⁺, and SiO⁻. The SiO molecule is experimentally known to exist in a singlet ${}^1\Sigma^+$ ground state with a bond length of 1.5097 Å and 1241.56-cm⁻¹ vibrational frequency.³¹ For SiO⁺, Huber and Herzberg³¹ suggest 1.519 Å as the bond length of the ground ${}^2\Sigma^+$ electronic state for which the experimental ionization potential is 11.6 ± 0.2 eV³² or 11.43 eV.³³ We optimized the

geometry of SiO at the MP2(full)/6-311+G* level and found an equilibrium bond length of 1.536 Å and a harmonic frequency of 1183 cm⁻¹.

The ionization energy of the 3σ -MO is smaller than that of the 1π -MO at Koopmans' approximation and in the OVGf and ADC-(3) methods. The vertical ionization energies IP(${}^2\Sigma^+$) = 11.7 ± 0.2 eV and IP(${}^2\Pi_i$) = 12.1 ± 0.3 eV can be considered as the recommended values derived from the results of the present ΔPMP4, ΔQCISD(T), ΔCISD(4), OVGf, and ADC(3) calculations (see Table 1). The former IP(${}^2\Sigma^+$) is in reasonable agreement with experimental data. Geometry relaxation does not change the lowest IP significantly, IP_a(${}^2\Sigma^+$) = 11.6 ± 0.2 eV; the adiabatic correction to the second IP is also small, IP_a(${}^2\Pi_i$) = 11.7 ± 0.2 eV. The optimized bond lengths and vibrational frequencies for these two cationic states are 1.534 Å and 1051 cm⁻¹ for SiO⁺ (${}^2\Sigma^+$) and 1.651 Å and 938 cm⁻¹ for SiO⁺ (${}^2\Pi_i$).

According to our calculations (Table 1), SiO has neither a positive vertical nor adiabatic electron affinity.

Si₂O, Si₂O⁺, and Si₂O⁻. Van Zee et al.³⁴ reported detection of SiSiO ($X^3\Sigma$) on the basis of their ESR spectra. However, DeKock et al.^{2a} have shown that the triplet SiOSi linear structure is more stable than the triplet SiSiO by ca. 10 kcal/mol using CISD/TZ+2P and CASSCF/TZ+2P methods. Recently Boldyrev and Simons^{2b} showed, at the QCISD(T)/6-311+G(2df) level, that indeed the ground state of this molecule has an angular singlet C_{2v} (1A_1) structure (see Figure 1) while the triplet structures are local minima and lie 18–27 kcal/mol higher. The latter calculations are sophisticated enough that new experimental studies on the structure of the Si₂O molecule should be considered.

The assignment of the ionization spectrum of Si₂O is unambiguous due to the significant gap (about 3.6 eV) between the lowest-energy 2A_1 (involving detachment of an electron from $4a_1$ -HOMO) and the next 2B_2 state. The $4a_1$ -MO is σ -bonding and π -bonding with respect to Si-Si, and its contributions from the oxygen atomic orbitals are modest. Therefore, after ionization, one expects elongation of the Si-Si bond length and a relatively small change in the Si-O bond lengths. The vibrational $\nu_1(a_1)$ and $\nu_2(a_1)$ frequencies in Si₂O⁺ (2A_1) which can be attributed to the Si-O stretch and Si-Si stretch are expected to be approximately the same as and lower than, respectively, the corresponding values in the neutral Si₂O molecule. Results of our calculations agree with this qualitative picture (see Figures 1 and 2).

The vertical IP_v(2A_1) of Si₂O is predicted to be 7.5 ± 0.2 eV on the basis of the five methods used, which is much lower than the IP = 11.7 eV of SiO. This is because ionization in Si₂O involves detachment of an electron from an orbital residing mainly on the silicon atoms, while in SiO, oxygen AOs also participate in the orbital. The geometric adiabatic correction to the first IP of Si₂O is relatively small (0.3 eV), and so our estimate for the adiabatic IP_a(2A_1) is 7.2 ± 0.2 eV. The second vertical IP_v(2B_2) of Si₂O is predicted to be 10.7 ± 0.2 eV, which is much higher than the first IP_v(2A_1). Geometry optimization, within C_{2v} symmetry, of Si₂O⁺(2B_2) leads to the linear SiOSi⁺ structure with a ($D_{\infty h}$, ${}^2\Pi_g$) final state. Therefore, the geometric adiabatic correction to this IP is very large (3.3 eV), and as a result, the adiabatic IP_a(${}^2\Pi_g$) is 7.4 ± 0.2 eV.

The lowest unoccupied $2b_1$ -MO has positive orbital energy, so the anion is predicted to be unstable at Koopmans' approximation. This $2b_1$ -MO is of π -MO character with bonding interaction with respect to both Si-O and Si-Si overlaps. However, Si atoms contribute more to this MO, so a larger change is expected in the Si-Si distance than in the Si-O bond lengths when this orbital is occupied. These qualitative predictions agree with the results of our calculations (Figure 1) for the Si-Si bond length, but we find the Si-O bond length also increases. The vertical EA_v(2B_1) is found to be 0.9 ± 0.2 eV (see Table 1) and its geometrical adiabatic correction is very small (0.1 eV), so our estimate of the adiabatic EA_a(2B_1) is 1.0 ± 0.2 eV. Our harmonic symmetric

$\nu_1(a_1) = 741 \text{ cm}^{-1}$ and $\nu_2(a_1) = 445 \text{ cm}^{-1}$ frequencies for Si_2O^- (2B_1) look reasonable, but the antisymmetric stretching frequency $\nu_3(b_2) = 3917 \text{ cm}^{-1}$ is overestimated again, probably due to symmetry breaking.

Si_3O , Si_3O^+ , and Si_3O^- . For the cation, anion, and neutral Si_3O , no experimental data are available. However, ab initio calculations of different geometric structures and electronic states for neutral Si_3O have been previously^{2b} performed, and a rhombus singlet structure C_{2v} (${}^1A_1, 1a_1^2 2a_1^2 1b_2^2 3a_1^2 1b_1^2 2b_2^2 4a_1^2 5a_1^2 2b_1^2 - 3b_2^2 1a_2^2$) has been found for the ground state (see Figure 1).

In this work, we optimized geometries of the Si_3O cationic 2B_1 ($1a_1^2 2a_1^2 1b_2^2 3a_1^2 1b_1^2 2b_2^2 4a_1^2 5a_1^2 2b_1^2$) and 2A_1 ($1a_1^2 2a_1^2 1b_2^2 3a_1^2 - 1b_1^2 2b_2^2 4a_1^2 2b_1^2 5a_1^2$) states and the anionic 2B_2 ($1a_1^2 2a_1^2 1b_2^2 3a_1^2 1b_1^2 2b_2^2 4a_1^2 5a_1^2 2b_1^2 3b_2^2$) and 2A_2 ($1a_1^2 2a_1^2 1b_2^2 3a_1^2 1b_1^2 2b_2^2 - 4a_1^2 2b_1^2 5a_1^2 1a_2^2$) states, the ion states having been identified on the basis of OVGf and ADC(3) calculations. The resulting geometrical structures and simulated IR spectra are given in Figures 1 and 2, respectively. According to our calculation, the vertical IPs and EAs (based on ΔPMP4 , $\Delta\text{QCISD}(4)$, OVGf, and ADC(3)) are $\text{IP}_v({}^2B_1) = 8.1 \pm 0.2 \text{ eV}$, $\text{IP}_v({}^2A_1) = 8.7 \pm 0.2 \text{ eV}$, $\text{EA}_v({}^2B_2) = 1.5 \pm 0.2 \text{ eV}$, and $\text{EA}_v({}^2A_2) = 0.6 \pm 0.2 \text{ eV}$ (see Table 1). For all four ionic states, the geometries do not differ significantly from the equilibrium geometry of the neutral Si_3O molecule (see Figure 1). Therefore, the corresponding adiabatic energy differences are $\text{IP}_a({}^2B_1) = 7.8 \pm 0.2 \text{ eV}$, $\text{IP}_a({}^2A_1) = 8.6 \pm 0.2 \text{ eV}$, $\text{EA}_a({}^2B_2) = 1.7 \pm 0.2 \text{ eV}$, and $\text{EA}_a({}^2A_2) = 0.7 \pm 0.2 \text{ eV}$.

Overview

In this study we used five sophisticated ab initio methods to calculate ionization potentials and electron affinities: ΔPMP4 , $\Delta\text{QCISD}(T)$, $\Delta\text{QCISD}(4)$, OVGf, and ADC(3). In the first three methods, the ionization energy is calculated through separate calculations on the neutral and ionic states, while two latter methods compute the ionization energy directly as a sum of electron relaxation and electron correlation corrections to the corresponding orbital energy. Both approaches have advantages and disadvantages. Indirect methods such as ΔMP4 and $\Delta\text{QCISD}(T)$ are based on the unrestricted Hartree-Fock reference wave function, and therefore the resulting wave function does not necessarily represent a pure spectroscopic state. Direct methods have no problems with the purity of the spectroscopic states, but current tools may be applied only for closed shell species whose ionization energies are to be computed. Therefore, in cases such as SiC, where the neutral and both ionic (positive and negative) states are open shell, direct methods are not applicable. Another disadvantage of the current direct methods is connected with the calculation of adiabatic IPs and EAs. However, promising results³⁵⁻³⁷ have recently appeared in the literature, where geometry optimization as well as frequency calculations are computed in direct methods. It seems that a combination of the direct and indirect methods is a powerful approach to examining the ionization processes.

Our ADC(3) calculations reveal for all the species studied here a breakdown of the one-electron picture of ionization for ionization energies larger than 11–12 eV, where many-body effects lead to satellite lines in the photoelectron spectra. The satellite lines should be more pronounced in the case of Si_2O and Si_3O than in the Si_2C and Si_3C because in Si_2O and Si_3O the LUMO and a few other unoccupied MOs are lower in energy than are the corresponding MOs in Si_2C and Si_3C .

Our calculations of the vertical IPs and EAs of SiC, Si_2C , Si_3C , SiO, Si_2O , and Si_3O agree among the five methods to within 0.5 eV. Our estimated first vertical IPs agree well with the experimental appearance potentials: $8.9 \pm 0.2 \text{ eV}$ vs $9.2 \pm 0.4 \text{ eV}^{23}$ and 9.0 eV^{24} for SiC, $9.1 \pm 0.2 \text{ eV}$ vs $9.2 \pm 0.3 \text{ eV}^{23}$ and 9.0^{24} for Si_2C , $8.1 \pm 0.2 \text{ eV}$ vs $8.2 \pm 0.3 \text{ eV}^{23}$ for Si_3C , and 11.7

$\pm 0.2 \text{ eV}$ vs $11.6 \pm 0.2 \text{ eV}^{32}$ and 11.42^{33} for SiO. We expect similar accuracy for the unknown Si_2O and Si_3O first IPs.

The IP = 11.7 eV of SiO is approximately 3 eV higher than the IP = 8.9 eV of SiC. SiO has no positive electron affinity while SiC has a large EA = 2.3 eV. In comparison, Si_2 has IP = 7.87 eV⁴⁰ and EA = 2.2 eV.²⁶

There are several interesting observations to be made relative to our calculated IPs and EAs of Si_nC and Si_nO and the available experimental data for pure silicon clusters.³⁸⁻⁴¹ The corresponding carbon clusters have linear geometries and therefore are not appropriate species for such comparison.

When another silicon atom is added to these clusters, things change; the IP = 7.2 eV of Si_2O is lower than the IP = 9.0 eV of Si_2C , and both of these molecules have electron affinities near 1 eV. The corresponding Si_3 cluster has IP = 7.9 eV⁴¹ and 8.14 eV⁴² and EA = 2.33 eV.⁴³

Adding yet another Si atom, one finds that both Si_3O and Si_3C have similar IPs (ca. 8 eV) and comparable EAs (ca. 1.5 eV; see Table 1), and that the corresponding Si_4 cluster has IP = 7.6 eV,⁴¹ 8.11 eV,⁴² and 7.3 eV⁴⁴ and EA = 2.15 eV.⁴³ The IP and EA values for Si_4 are close to the corresponding values for Si_3O and Si_3C , which implies that ionization and electron capture in Si_3C and Si_3O involve primarily the silicon part of the cluster.

As the number of silicon atoms increases in Si_nX species, where X is a more electronegative atom than silicon, we expect that the ionization potentials and electron affinities will become closer to the corresponding values of pure silicon clusters, Si_n . It follows from our calculations that this is the case even for rather small ($n \geq 3$) clusters.

Conclusions

(1) The results of our IP calculations for SiC, Si_2C , Si_3C , and SiO agree within 0.3 eV with experimental data and among all five of our methods— ΔPMP4 , $\Delta\text{QCISD}(T)$, $\Delta\text{QCISD}(4)$, OVGf, and ADC(3)—to within 0.5 eV.

(2) We have made new predictions of the vertical and adiabatic IPs and EAs of SiC, Si_2C , Si_3C , SiO, Si_2O , and Si_3O . For the neutral and ionic states of these species, we calculated the infrared spectra to assist in identification of these species in the gas-phase or matrix isolation.

(3) We infer that electron removal or electron attachment in Si_3C and Si_3O involves the silicon part of the clusters because the corresponding ionization energies are close to the corresponding values for Si_4 . In contrast, for Si_2C , Si_2O , SiC, and SiO, the IPs and EAs are very different from the corresponding numbers for Si_3 and Si_2 .

(4) Our ADC(3) calculations reveal breakdown of the one-electron picture of ionization at ionization energies higher than 11–12 eV where many-body effects lead to satellite lines in the photoelectron spectra. The satellite lines should be more pronounced in the case of Si_2O and Si_3O than in Si_2C and Si_3C .

Acknowledgment. This work was facilitated by an Alexander von Humboldt Fellowship to V.G.Z. and was supported in part by the Office of Naval Research and by National Science Foundation Grant No. CHE9116286 in Utah. The authors thank D. A. Boldyrev for coding the program for drawing the simulated IR spectra.

References and Notes

- (1) (a) Grev, R. S.; Schaefer, H. F., III. *J. Chem. Phys.* **1985**, *82*, 4126. (b) Bolton, E. E.; DeLeeuw, B. J.; Fowler, J. E.; Grev, R. S.; Schaefer, H. F., III. *J. Chem. Phys.* **1992**, *97*, 5586. (c) Rittby, C. M. L. *J. Chem. Phys.* **1991**, *95*, 5609. (d) Rittby, C. M. L. *J. Chem. Phys.* **1992**, *96*, 6768.
- (2) (a) DeKock, R. L.; Yates, B. F.; Schaefer, H. F., III. *Inorg. Chem.* **1989**, *28*, 1680. (b) Boldyrev, A. I.; Simons, J. *J. Phys. Chem.* **1993**, *97*, 5875.
- (3) Schlegel, H. B. *J. Comput. Chem.* **1982**, *3*, 214.
- (4) Firsich, M. J.; Trucks, G. W.; Head-Gordon, M.; Gill, P. M. W.; Wong, M. W.; Foresman, J. B.; Johnson, B. G.; Schlegel, H. B.; Robb, M. A.; Replogle, E. S.; Gomperts, R.; Andres, J. L.; Raghavachari, K.; Binkley,

J. S.; Gonzales, C.; Martin, R. L.; Fox, D. J.; DeFrees, D. J.; Baker, J.; Stewart, J. J. P.; Topiol, S.; Pople, J. A. *GAUSSIAN 92*, Revision C; Gaussian Inc.: Pittsburgh, PA, 1992.

(5) (a) Frisch, M. J.; Pople, J. A.; Binkley, J. S. *J. Chem. Phys.* **1984**, *80*, 3265. (b) Krishnan, R.; Binkley, J. S.; Seeger, R.; Pople, J. A. *J. Chem. Phys.* **1980**, *72*, 650.

(6) Clark, T.; Chandrasekhar, J.; Spitznagel, G. W.; Schleyer, P. v. R. *J. Comput. Chem.* **1983**, *4*, 294.

(7) McLean, A. D.; Chandler, G. S. *J. Chem. Phys.* **1980**, *72*, 5639.

(8) Krishnan, R.; Pople, J. A. *Int. J. Quantum Chem.* **1978**, *14*, 91.

(9) Pople, J. A.; Head-Gordon, M.; Raghavachari, K. *J. Chem. Phys.* **1987**, *87*, 5968.

(10) Schlegel, H. B. *J. Chem. Phys.* **1984**, *84*, 4530.

(11) Cederbaum, L. S. *Theor. Chim. Acta* **1973**, *31*, 239.

(12) Cederbaum, L. S. *J. Phys.* **1975**, *B8*, 290.

(13) Cederbaum, L. S.; Domcke, W. In *Advances in Chemical Physics*; Prigogine, I., Rice, S. A., Eds.; Wiley: New York, 1977; Vol. 36, p 205.

(14) Schirmer, J.; Cederbaum, L. S. *J. Phys.* **1978**, *B11*, 1889. Schirmer, J.; Cederbaum, L. S.; Walter, O. *Phys. Rev.* **1983**, *A28*, 1237.

(15) Niessen, W. von; Schirmer, J.; Cederbaum, L. S. *Comput Phys. Rep.* **1984**, *1*, 57.

(16) Schirmer, J.; Angonoa, G. *J. Chem. Phys.* **1989**, *91*, 1754.

(17) Anderson, K.; Blombeg, M. R. A.; Fulscher, M. P.; Kello, V.; Lindh, R.; Malmqvist, P.-A.; Noga, J.; Olsen, J.; Roos, B. O.; Sadlej, A. J.; Siegbahn, P. E. M.; Urban, M. *MOLCAS-2*, Version 2; University of Lund, Sweden and Widmark, P.-O. IBM, Sweden, 1991.

(18) Widmark, P.-O.; Malmqvist, P.-A.; Roos, B. O. *Theor. Chim. Acta* **1990**, *77*, 291. Widmark, P.-O.; Persson, B. J.; Roos, B. O. *Theor. Chim. Acta* **1991**, *79*, 419.

(19) Almlof, J.; Taylor, P. R. *J. Chem. Phys.* **1987**, *86*, 4070.

(20) Davidson, E. R. In *The World of Quantum Chemistry*; Daudel, R., Ed.; Reidel: Dordrecht, 1974; p 17. Langhoff, S. R.; Davidson, E. R. *Int. J. Quantum Chem.* **1974**, *8*, 61.

(21) (a) Bernath, P. F.; Rogers, S. A.; O'Brien, L. C.; Barzier, C. R.; McLean, A. D. *Phys. Rev. Lett.* **1988**, *60*, 197. (b) Brazier, C. R.; O'Brien, L. C.; Bernath, P. F. *J. Chem. Phys.* **1989**, *91*, 7384. (c) Ebben, M.; Drabbels, M.; Meulen, J. J. *J. Chem. Phys.* **1991**, *95*, 2292.

(22) (a) Bruna, P. J.; Peyrimhoff, S. D.; Buenker, R. J. *J. Chem. Phys.* **1980**, *72*, 5437. (b) Rohlfing, C. M.; Martin, R. L. *J. Phys. Chem.* **1986**, *90*, 2043. (c) Bauschlicher, C. W., Jr.; Langhoff, S. R. *J. Chem. Phys.* **1987**, *87*, 2919. (d) Martin, J. M. L.; Francois, J. P.; Gijbels, R. *J. Chem. Phys.* **1990**, *92*, 6655. (e) McLean, A. D.; Liu, B.; Chandler, G. S. *J. Chem. Phys.* **1992**, *97*, 8459.

(23) Drowart, J.; De Maria, G.; Inghram, M. G. *J. Chem. Phys.* **1958**, *29*, 1015.

(24) Verhaegen, G.; Stafford, F. E.; Drowart, J. *J. Chem. Phys.* **1964**, *40*, 1622.

(25) (a) Ervin, K. M.; Lineberger, W. C. *J. Phys. Chem.* **1991**, *95*, 1167. (b) Arnold, D. W.; Bradforth, S. E.; Kitsopoulos, T. N.; Neumark, D. M. *J. Chem. Phys.* **1991**, *95*, 8753.

(26) (a) Kitsopoulos, T. N.; Chick, C. J.; Zhao, Y.; Neumark, D. M. *J. Chem. Phys.* **1991**, *95*, 1441. (b) Nimlos, M. R.; Harding, L. B.; Ellison, G. B. *J. Chem. Phys.* **1987**, *87*, 5116.

(27) Weltner, W. Jr.; Mcleod, D., Jr. *J. Chem. Phys.* **1964**, *41*, 235.

(28) Kafafi, Z. H.; Hauge, R. H.; Fredin, L.; Margrave, J. L. *J. Phys. Chem.* **1983**, *87*, 797.

(29) Presilla-Márquez, J. D.; Graham, W. R. M. *J. Chem. Phys.* **1991**, *95*, 5612.

(30) Presilla-Márquez, J. D.; Graham, W. R. M. *J. Chem. Phys.* **1992**, *96*, 6509.

(31) Huber, K. P.; Herzberg, G. *Molecular Spectra and Molecular Structure Constants of Diatomic Molecules*; van Nostrand Reinhold Publishing Co.: New York, 1979.

(32) Hildenbrand, D. L.; Murad, E. *J. Chem. Phys.* **1969**, *51*, 807.

(33) Lias, S. G.; Bartmess, J. E.; Liebman, J. F.; Homes, J. L.; Levin, R. D.; Mallard, W. G. *J. Phys. Chem. Ref. Data* **1988**, *17*, 635; Suppl. 1, *Gas Phase Ion and Neutral Thermochemistry*.

(34) Van Zee, R. J.; Ferrante, R. F.; Weltner, W., Jr. *Chem. Phys. Lett.* **1987**, *139*, 426.

(35) Ortiz, J. V. *Int. J. Quantum Chem.* **1992**, *26*, 1.

(36) Cioslowski, J.; Ortiz, J. V. *J. Chem. Phys.* **1992**, *96*, 8379.

(37) Ortiz, J. V. *J. Chem. Phys.* **1992**, *97*, 7531.

(38) Franklin, J. L.; Dillard, J. G.; Rosenstock, H. M.; Herron, J. T.; K. Draxl, K.; Field, F. H. *Ionization Potentials, Appearance Potentials, and Heats of Formation of Gaseous Positive Ions*; National Standard Reference Data Series; National Bureau of Standards: Washington, DC, 1969.

(39) Trevor, D. J.; Cox, D. M.; Reichmann, K. C.; Brikman, R. O.; Kaldor, A. *J. Phys. Chem.* **1987**, *91*, 2598.

(40) Yang, S.; Taylor, K. J.; Craycraft, M. J.; Conceicao, J.; Pettiette, C. L.; Cheshnovsky, O.; Smalley, R. E. *Chem. Phys. Lett.* **1988**, *144*, 431.

(41) Raghavachari, K.; Logovinsky, V. *Phys. Rev. Lett.* **1985**, *55*, 2853.

(42) Niessen, W. von; Zakrzewski, V. G. *J. Chem. Phys.* **1993**, *98*, 1271.

(43) Kitsopoulos, T. N.; Chick, C. J.; Weaver, A.; Neumark, D. M. *J. Chem. Phys.* **1990**, *93*, 6108.

(44) Balasubramanian, K. *Chem. Phys. Lett.* **1987**, *135*, 283.